JCB Article

# Gliotactin, a novel marker of tricellular junctions, is necessary for septate junction development in *Drosophila*

**Joost Schulte,[1] Ulrich Tepass,[2] and Vanessa J. Auld[1]**

[1]Department of Zoology, University of British Columbia, Vancouver, BC, V6T 1Z4, Canada
[2]Department of Zoology, University of Toronto, Toronto, ON, M5S 3G5, Canada

Septate junctions (SJs), similar to tight junctions, function as transepithelial permeability barriers. Gliotactin (Gli) is a cholinesterase-like molecule that is necessary for blood–nerve barrier integrity, and may, therefore, contribute to SJ development or function. To address this hypothesis, we analyzed Gli expression and the *Gli* mutant phenotype in *Drosophila* epithelia. In *Gli* mutants, localization of SJ markers neurexin-IV, discs large, and coracle are disrupted. Furthermore, SJ barrier function is lost as determined by dye permeability assays. These data suggest that Gli is necessary for SJ formation. Surprisingly, Gli distribution only colocalizes with other SJ markers at tricellular junctions, suggesting that Gli has a unique function in SJ development. Ultrastructural analysis of *Gli* mutants supports this notion. In contrast to other SJ mutants in which septa are missing, septa are present in *Gli* mutants, but the junction has an immature morphology. We propose a model, whereby Gli acts at tricellular junctions to bind, anchor, or compact SJ strands apically during SJ development.

## Introduction

Permeability barriers have important roles in many tissues in both vertebrates and invertebrates. The blood–brain barrier, for example, is essential in vertebrates to keep the brain isolated from blood-borne growth factors, neural active compounds, and fluctuating blood ion levels that can severely impact neuronal physiology and brain function (Rubin and Staddon, 1999). Similarly, in insects, the high potassium concentration of the hemolymph can block action potentials in neurons, and, thus, cause paralysis, if the blood–brain barrier is disrupted (Auld et al., 1995; Baumgartner et al., 1996). Epithelial permeability barriers are formed by tight junctions (TJs)* in chordates and by septate junctions (SJs) in most invertebrates. TJs and SJs differ in their ultrastructure, position in epithelial cells, and molecular composition, yet they share certain organizational similarities that enables them to form effective permeability barriers (Lane et al., 1994; Tepass et al., 2001; Tsukita et al., 2001).

SJs are located in the apical portion of the lateral membrane of invertebrate epithelial cells, immediately below adherens junctions (AJs). TJs in contrast, lie apical to AJs in vertebrate epithelial cells. SJs are characterized by a ladderlike array of cross-bridges or septa that span the 15–20-nm intermembrane space of cell–cell contacts. TJs, on the other hand, appear as multiple "kissing-points," in transmission electron micrographs where adjacent plasma membranes are in direct contact (Lane et al., 1994; Tsukita et al., 2001). Both SJs and TJs are composed of multiple strands with some variation in strand number depending on cell type. For example, 10 or more strands typically compose an SJ in a locust epithelial cell, whereas 4–7 strands are found in a TJ of kidney distal tubule epithelial cell. SJ strands are tightly arrayed parallel to each other, whereas TJ strands are less compact and are organized into overlapping or anastomizing networks (Claude and Goodenough, 1973; Lane and Swales, 1982). The multistranded composition of both SJs and TJs appears to be necessary to effectively block the paracellular flow of substances. In insects, permeability studies have shown that heavy metal tracer dyes are often able to penetrate deep into the stacked arrays of SJ strands before they are blocked from paracellular passage (Swales and Lane, 1985). Similarly, studies of "tight" and "leaky" TJs in vertebrate epithelia have shown a positive

Address correspondence to Vanessa J. Auld, Dept. of Zoology, University of British Columbia, 6270 University Blvd., Vancouver, BC, V6T 1Z4, Canada. Tel.: 604-822-1977. Fax: 604-822-2416. E-mail: auld@zoology.ubc.ca

*Abbreviations used in this paper: AJ, adherens junction; arm, Armadillo; β-Gal, β-galactosidase; BNB, blood–nerve barrier; Cora, coracle; Dlg, discs large; Dnl, *Drosophila* neuroligin; Gli, gliotactin; IMP, intermembrane particle; Nrx, neurexin-IV; PDZ, PSD-95/Dlg/ZO-1; pSJ, pleated SJ; Scrib, scribble; SJ, septate junction; sSJ, smooth SJ; TCD, tricellular channel diaphragm; TCP, tricellular plug; TEM, transmission EM; TJ, tight junction.

Key words: epidermis; epithelial cells; electrotactin; neuroligin; neurexin

correlation between strand number and TJ permeability (Claude and Goodenough, 1973).

In *Drosophila*, two types of SJs, smooth (sSJs) and pleated SJs (pSJs), have been observed (Tepass and Hartenstein, 1994). Smooth SJs and pSJs vary morphologically and have different tissue distributions, but they are functionally equivalent (Lane et al., 1994). In freeze-fracture electron micrographs, pSJ strands appear to lie in membrane depressions or grooves that are absent in sSJs (Lane and Swales, 1982). pSJs are found in ectodermally derived tissue, such as the foregut, hindgut, tracheae, and glia, whereas sSJs are found in endodermally derived tissue, such as the midgut (Tepass and Hartenstein, 1994).

TJs and SJs have been described to encircle epithelial cells as a continuous belt, though this view has been challenged. EM studies of epithelial cells, in both vertebrates and insects, have shown that the continuity of TJ and SJ belts is interrupted at sites of tricellular contact by "pores" or "channels" that span the depth of the epithelium (Fristrom, 1982; Graf et al., 1982; Noirot-Timothée et al., 1982; Walker et al., 1985). It is unclear what the function of these specialized structures may be. In insects, it has been proposed that diaphragms associated with these channels may serve as anchors for SJ strands (Fristrom, 1982; Graf et al., 1982; Noirot-Timothée et al., 1982). Similarly, developmental studies on rat olfactory epithelium suggest that de novo synthesis of TJs strands may occur at sites of tricellular contact (Menco, 1988). Recent studies on human umbilical vein cultures have suggested that the localized disruption of TJs at endothelial tricellular corners is important during acute immune responses as it enables neutrophils to migrate across capillaries and reach sites of inflammation or infection (Burns et al., 2000).

To more thoroughly appreciate the similarities and differences between vertebrate TJs and *Drosophila* SJs, a molecular characterization of these junctions has been performed over the last decade. Of the *Drosophila* SJ–associated proteins, four have clear roles in SJ formation. Mutations in *neurexin-IV (Nrx), discs large (Dlg), scribble (Scrib),* or *coracle (Cora)* prevent the formation of septa (Baumgartner et al., 1996; Woods et al., 1996; Lamb et al., 1998; Bilder et al., 2003). *Nrx* is a transmembrane protein and a member of the neurexin family of synapse-associated proteins (Ushkaryov et al., 1992; Baumgartner et al., 1996). Dlg and Scrib are cytosolic, PSD-95/Dlg/ZO-1 (PDZ) domain-containing proteins that also have roles in establishing epithelial cell polarity before SJ development (Perrimon, 1988; Woods et al., 1996; Bilder and Perrimon, 2000; Bilder et al., 2003). Cora is a band 4.1–related protein that possesses a four point one/ezrin/vadixin/moesin domain and physically associates with Nrx (Fehon et al., 1994; Ward et al., 1998). In the case of vertebrate TJs, at least 25 claudins have been identified that are believed to play critical roles in TJ development (Furuse et al., 1998; Gow et al., 1999; Morita et al., 1999; Tsukita and Furuse, 2000). Claudins can interact in a homophilic or heterophilic fashion, and their mixing ratio is believed to moderate the permeability of TJ transepithelial barriers (Furuse et al., 1999). In addition, numerous other transmembrane or cytoplasmic factors have been found to be associated with TJs (Tsukita et al., 2001).

No significant similarities between the molecular composition of vertebrate TJs and *Drosophila* SJs have been noted so far (Tepass et al., 2001). Moreover, vertebrate homologues of *Drosophila* Nrx and Cora have been identified that localize to mammalian paranodal junctions, at the interface of axons and glia (Menegoz et al., 1997; Poliak et al., 1999; Bhat et al., 2001; Boyle et al., 2001). These junctions are morphologically very similar to *Drosophila* SJs. It is important to more thoroughly characterize SJs, TJs, and paranodal junctions, in order to establish a better understanding of the relationship between these junction types and to gain insight into the mechanism of permeability barrier formation.

Gliotactin (Gli) is a noncatalytically active cholinesterase-like molecule that is a member of a class of adhesion proteins termed the electrotactins (Auld et al., 1995, Botti et al., 1998). In the peripheral nervous system, Gli is necessary for glial ensheathment of axons, and for the formation of the glial-based blood–nerve barrier (BNB; Auld et al., 1995). Although pSJs between glial wraps constitute the molecular seal of the BNB, it has not been determined if the BNB defects seen in *Gli* mutants arises from defective pSJ development or from inadequate axonal ensheathment (Baumgartner et al., 1996; for review see Carlson et al., 2000). Here, we investigate the role of Gli in the formation of SJs through genetic and cell biological approaches.

## Results

### Expression profile of Gli in the epidermis

To test the hypothesis that Gli is involved in the formation of SJs, we first examined if the tissue and subcellular distribution of Gli matches that reported for SJs (Fehon et al., 1994; Tepass and Hartenstein, 1994; Baumgartner et al., 1996; Lamb et al., 1998). Embryos were doubled labeled for Gli and the pSJ markers Nrx and Cora to investigate their temporal and spatial overlap. Gli first appears in the ectoderm at stage 11 of embryogenesis, shortly after Nrx, and persists throughout embryonic development (Fig. 1). Gli expression at this stage appears to be due to zygotic gene activity as no maternal *Gli* mRNA is detected in Northern blots of 0–6-h embryos (stage 1–10; unpublished data). The distribution of Gli and Nrx protein is similar in the epidermis at stage 11, and both molecules are distributed evenly over the lateral membrane of epithelial cells (Fig. 1 A). In the homozygous *Gli* mutants ($Gli^{AE2\Delta45}$, $Gli^{AE2\Delta4b}$, $Gli^{DV3}$, and $Gli^{CQ1}$), no Gli staining was observed at any stage of embryogenesis (Fig. 1 E) demonstrating that the Gli 1F61D4 mAb is specific to Gli.

At stage 13, the localization of Nrx and Gli changes. In en face views of the epidermis, Gli becomes concentrated at the tricellular corners of abutting epithelial cells, whereas Nrx remains distributed around the cell circumferences (Fig. 1 B, arrowhead). Occasionally, patchy Gli staining is observed in some of the elongated epithelial cells in the dorsal epidermis (Fig. 1 B, solid arrow). Interestingly, at the leading edge of the epidermis there is little overlap between Gli and Nrx staining (Fig. 1 B, concave arrow). In the amnioserosa, Gli and Nrx staining is absent, consistent with the fact that this tissue lacks SJs (Tepass and Hartenstein, 1994). In addition to the epidermis, Gli

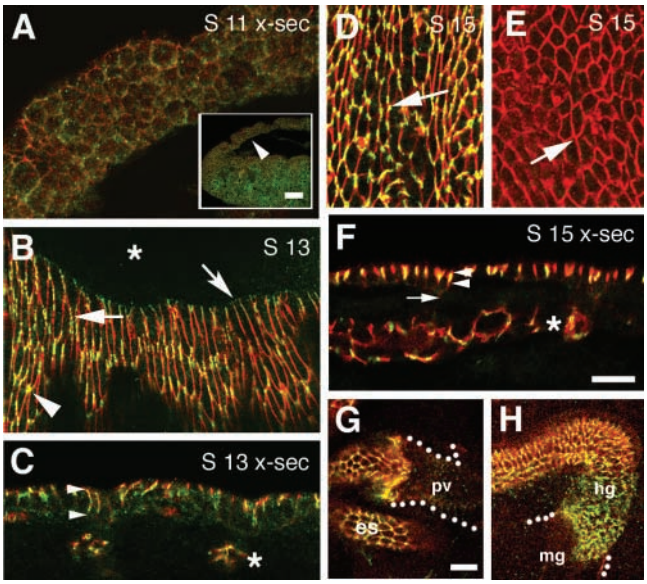


Figure 1. **Gli is expressed in the epidermis and it is localized to the tricellular corners of abutting epithelial cells.** (A–H) Whole mount embryos of different developmental stages are shown double stained for Gli (green), and either the (A–F) pSJ protein Nrx or (G and H, red) Cora. The overlap of Gli and Nrx, or Cora, is yellow. Images are of wild-type embryos, with the exception of E, which is a $Gli^{AE2\Delta45}$-null mutant. (A) High magnification view of the epidermis (cross section view) of a stage 11 embryo taken at the position of the arrowhead in the low-magnification inset. At this stage, the distribution of Gli is quite uniform around the surface of the epithelial cells and similar to that of Nrx. (B) En face view of a stage 13 embryo undergoing dorsal closure. The localization profile for Gli is variable. At the leading edge (concave arrow), Gli diffusely labels epithelial cell membranes as they make contact with the underlying amnioserosa (asterisk). Epithelial cells in more ventral positions, have Gli concentrated in patches around their circumferences (solid arrow), or localized to tricellular corners (arrowhead). Gli distribution is distinct, although overlapping, with that of Nrx. The amnioserosa lacks both Gli and Nrx expression (asterisk). (C) Cross section of a stage 13 embryo. Gli expression is restricted to the lateral membrane of epithelial cells (region between arrowheads), and is concentrated in patches. Gli staining in the tracheae underlying the epidermis is also evident (asterisk). (D) En face view of epidermis of a stage 15 embryo. Gli remains concentrated at tricellular junctions (arrow). (E) En face view of a stage 15 $Gli^{AE2\Delta45}$-null mutant, double stained for Gli and Nrx. In the absence of Gli protein, the Gli mAb does not stain the tricellular corners of the epidermis (arrow) and, thus, it is specific to a Gli epitope. (F) Cross section of the epidermis of a stage 15 embryo. Gli localization is restricted to the apical portion of the lateral membrane domain and lies within the Nrx-positive SJ domain (arrowheads). Gli expression does not extend to the bottom of epithelial cells (arrow). Gli is only sporadically seen in the lateral membrane of epithelium because the plane of section only occasionally transects a tricellular corner. Gli expression in tracheae persists (asterisk). (G) Gli expression is evident in the esophagus (es) as is Cora. Both proteins are absent from the outer layer of the proventriculus (pv, dotted line). (H) Gli and Cora are expressed in the hindgut (hg), but absent from midgut (mg). Bars: (A, inset) 50 μm; (F and G) 10 μm.

is also found at the tricellular junctions of all epithelial tissues that express Nrx and Cora, and in which pSJs have been observed at the EM level (Fehon et al., 1994; Tepass and Hartenstein, 1994; Baumgartner et al., 1996; Lamb et al., 1998). These tissues include the trachea (Fig. 1 F, asterisk), salivary glands (see Fig. 5), PNS glia (Auld et al., 1995), the chordotonal organs (unpublished data), and the foregut and the hindgut (Fig. 1, G and H). Gli was not observed in tissues that contain sSJs.

In addition to becoming redistributed in the planar axis of epithelial cells, Gli also undergoes a redistribution along the apical–basal axis. At stage 13 of embryogenesis, Gli is localized along the entire length of the lateral membrane. However, unlike Nrx, Gli is typically concentrated in multiple discrete patches within the lateral membrane (Fig. 1 C). By stage 15 of embryogenesis, Gli expression is restricted to the apical half of the lateral membrane where it colocalizes with Nrx at the presumptive pSJ domain (Fig. 1 F). The tissue distribution and subcellular localization profile of Gli suggest that it is a component of pSJs, but its unique localization to tricellular junctions suggests that it plays a distinct role from Nrx and Cora.

## SJ markers are mislocalized in *Gli* mutants

To investigate the effect of loss of Gli on epithelial cell development, we stained homozygous *Gli* mutants for a variety of epithelial markers. We focused on stage 15 embryos that in wild-type display the mature distribution pattern of SJ markers. Four different strong *Gli* loss of function alleles ($Gli^{AE2\Delta45}$, $Gli^{AE2\Delta4b}$, $Gli^{DV3}$, and $Gli^{CQ1}$) were tested and gave indistinguishable results.

Epidermal cells within the abdominal segments of *Gli* mutants are slightly taller and have a more uniformly columnar appearance than wild-type cells as revealed through α-spectrin labeling, which outlines cell profiles (Fig. 2, A and B). Next, we double stained *Gli* mutant embryos for SJ and AJ markers. In stage 15 *Gli* mutants, the SJ markers Dlg, Nrx, and Cora are all mislocalized (Fig. 2, C–H). Rather than being confined to the apical half of the lateral membrane, these SJ markers extend to the extreme basal side of epithelial cells, although an apical emphasis in their distribution is retained (Fig. 2, D, F, and H). The mislocalization of Dlg is less severely affected than that of Cora or Nrx in *Gli* mutants. Failure of SJ markers to redistribute to the apico-lateral membrane is already seen at stage 13, at a time when the first septa appear in wild-type embryos (Tepass and Hartenstein, 1994). In contrast to SJ markers, AJ markers (Armadillo [arm] and DE-cadherin) are normally localized in *Gli* mutants (Fig. 2, C–F and G and H, respectively). Together, the generally normal columnar morphology of epithelial cells seen in *Gli* mutants, and the correct apical localization of AJ markers suggests that Gli does not have a significant role in specifying apical–basal epithelial polarity. However, the mislocalization of SJ markers in *Gli* mutants indicates that Gli has a specific role in the maturation of pSJs.

*Nrx* and *Cora* mutant embryos have defects in dorsal closure, which manifest as dorsal holes or scabs in cuticle preparations (Baumgartner et al., 1996; Lamb et al., 1998). In *Gli* mutants, cuticles appear normal, however, small dorsal "holes" are observed at a low frequency in the epidermis of stage 16 embryos (unpublished data). These observations suggest that dorsal closure is delayed in some *Gli* mutant embryos; however, it is completed successfully before cuticle deposition.

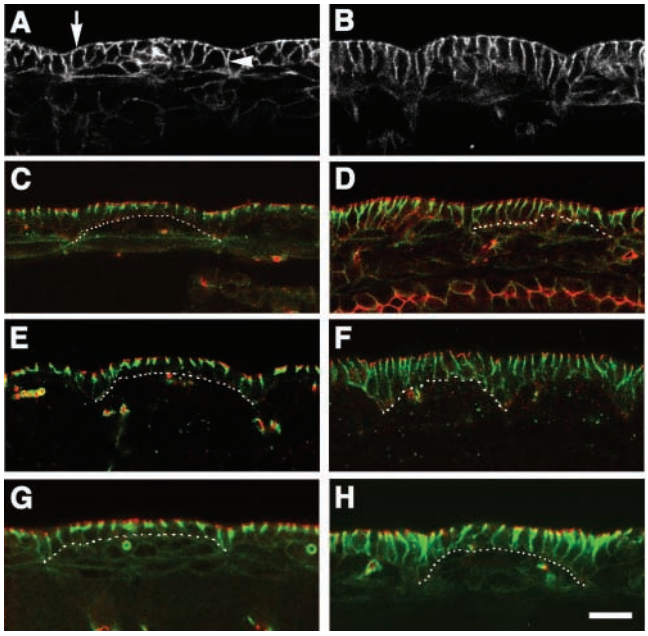


Figure 2. **SJ markers are mislocalized in *Gli* mutants.** All images are of stage 15 embryos and the epidermis is viewed in cross section. (A, C, E, and G) Wild-type embryos. (B, D, F, and H) Homozygous $Gli^{AE2\Delta45}$ mutants. (A and B) α-Spectrin staining reveals general epithelial morphology. Wild-type epithelial cells have columnar morphology, and α-spectrin labels both the (A, arrow) apical and (B, arrowhead) lateral membrane domains. In *Gli* mutants, epithelial cells are slightly taller and have a more uniform columnar shape, whereas the localization pattern of α-spectrin is (B) wild type. (C and D) Embryo stained for the SJ marker, Dlg (green) and the AJ marker; arm (red). The dotted line marks the basal surface of epithelial cells in a single abdominal segment. The stereotypic organization of AJs positioned apical to pSJs can be observed in (C) wild-type embryos. In *Gli* mutants, Dlg localization is disrupted and has diffused basally, whereas arm localization is (D) normal. (E and F) Embryos doubled stained for the pSJ marker Nrx (green) and arm (red). Nrx is also mislocalized in (F) *Gli* mutants. (G and H) Embryos stained for the pSJ marker Cora (green) and the AJ marker DE-cad (red). Just like Dlg and Nrx, the pSJ marker Cora is mislocalized in *Gli* mutants; however, the localization of DE-cad is (H) unaffected. Bar, 10 μm.

## Gli's localization at epidermal tricellular corners is dependent on Nrx

To determine if pSJ formation is necessary for Gli to become localized to the tricellular corners of epithelial cells, Gli distribution in $Nrx^{46}$ homozygous mutants was analyzed. $Nrx^{46}$ is a severe loss of function mutation and septae are absent from pSJs in these mutants (Baumgartner et al., 1996). We found that Gli does not localize normally to the tricellular corners of epithelial cells in late $Nrx^{46}$ mutant embryos (Fig. 3). In en face views of the epidermis of stage 15, $Nrx^{46}$ mutants with a severe dorsal closure phenotype, Gli is abnormally distributed around the circumference of cells (Fig. 3 C). Similarly, in cross section views of these mutants, Gli is not restricted to the apical half of lateral membrane, but instead extends basally (Fig. 3 D). In stage 15, $Nrx^{46}$ mutants with mild dorsal closure phenotypes, Gli is less severely mislocalized (Fig. 3, E and F). Thus, the severity of the dorsal closure phenotype in the $Nrx^{46}$ mutants correlates with the severity of Gli mislocalization in the epithelium. The localization profile of Gli in stage 15 $Nrx^{46}$ mutants resembles that of Gli in wild-type embryos at stage 13 of development (compare Fig. 1 B with Fig. 3, C and E; compare Fig. 1 C with Fig. 3, D and F). These results indicate a reciprocal dependence between Gli and Nrx for localization, but also suggest that pSJs must develop to enable Gli to localize to tricellular junctions.

## pSJ septae are present in *Gli* mutants, but not compacted into clusters

Ultrastructural analysis of *Gli* mutants was performed to further characterize the nature of the pSJ defect. We examined pSJ structure at bicellular contacts, as well as at tricellular junctions, in the epidermis (Fig. 4). In wild-type animals pSJ septa are present in the apical 1/3 to 2/3 of the lateral membrane and are typically organized into clusters (Fig. 4 A). We counted the number of pSJ septa, and the number of clusters of septa per cell–cell contact in stage 17, wild-type, and *Gli* mutant embryos. It was discovered that total number of septa at a cell–cell contact is statistically equivalent in wild-type and *Gli* mutants; however, there are more clusters containing fewer septa/cluster in *Gli* mutants (Fig. 4, A, C, and E). 16.4 septa/cell–cell contact (SD 7.2, $n = 47$) occur in wild-type animals, as compared with 15.5 septa/cell–cell contact in *Gli* mutants (SD 5.3, $n = 98$). 3.3 (SD 1.7) sep-

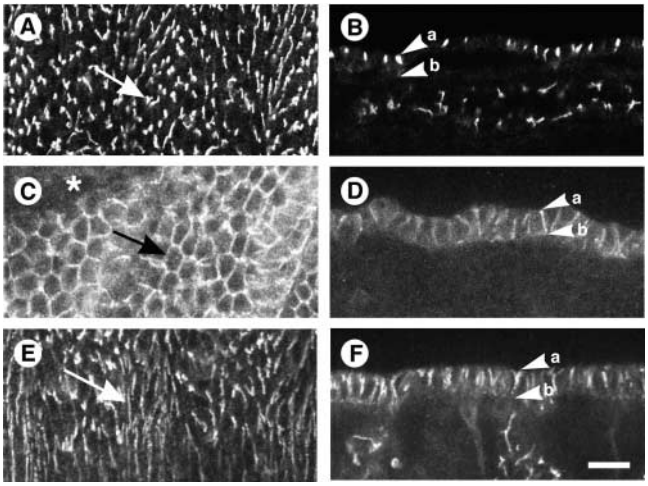


Figure 3. **Gli localization at epithelial tricellular corners is dependent on Nrx.** All embryos are stained for Gli and are at stage 15 of development. (A and B) Wild-type embryos. (C–F) $Nrx^{46}$ homozygous mutant embryos. (A) Gli localizes to the tricellular corners (arrow) of epithelial cells (en face view). (B) Gli, at tricellular corners, is restricted to the apical half of the lateral membrane domain (cross section view). The apical (a) and basal (b) surfaces of an epithelial cell are marked. (C and D) Severe $Nrx^{46}$ homozygous mutant embryo. (C) Gli fails to localizes to the tricellular corners of epithelial cells (arrow) and is distributed around the circumference (en face view). In this late stage embryo, dorsal closure has failed (asterisk). (D) Cross section view of the epidermis in C. Rather than being restricted to the apical half of the lateral membrane, Gli extends to the basal surface. (E and F) $Nrx^{46}$ homozygous mutant embryo with a weak dorsal closure phenotype. (E) En face view of the epidermis. In these mutants, the epidermis appears more wild type, but Gli does not localize to tricellular corners (arrow). (F) Cross section view of the epidermis in E. As in D, Gli is not concentrated to the pSJ domain at tricellular corners, but diffuses basally. Bar, 10 μm.

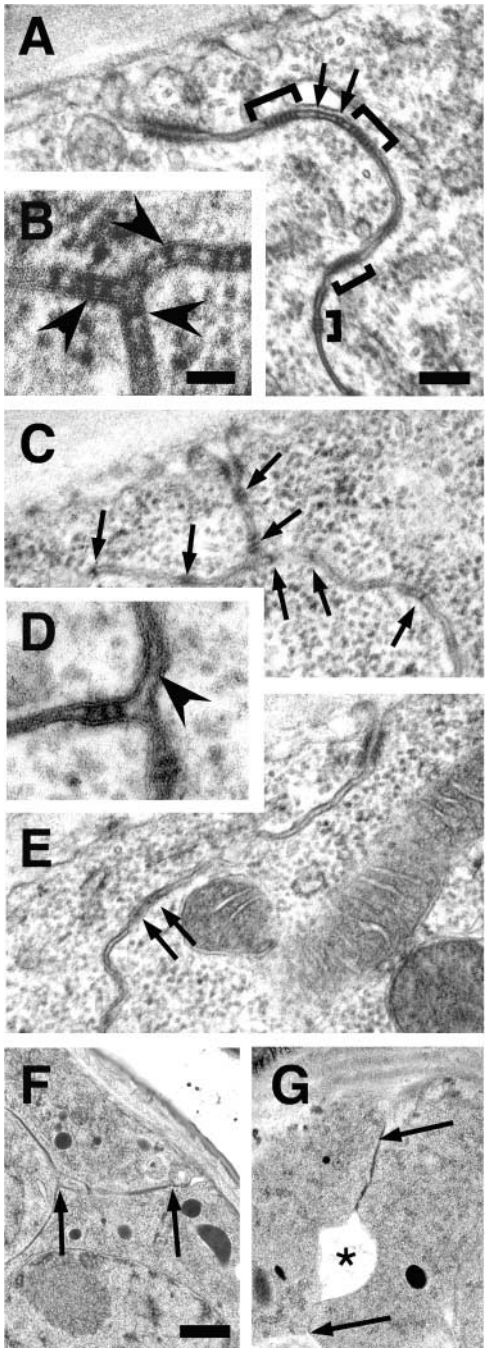


Figure 4. **TEM of stage 17 *Gli* mutant embryos reveals that pSJ septae are not tightly arrayed.** (A,B, and F) Wild-type epidermis. (C–E and G) $Gli^{\Delta E2\Delta 45}$ mutant epidermis. (A) pSJs typically contain clusters of septae (brackets) interspersed with single or pairs of septa (arrows). (B) At tricellular junctions, pSJ septae are present at all bicellular contacts (arrowheads). (C and E) In *Gli* mutants, single or pairs of pSJ septa predominate (arrows), and few clusters are evident. (D) pSJ septa are not present at all bicellular contacts of tricellular junctions in *Gli* mutants (arrowhead). (F and G) Embryos prepared for TEM analysis with high pressure freezing. (F) In wild type, neighboring epidermal cells contact each other over the length of the lateral membrane (region between arrows). (G) In *Gli* mutants, large regions of delamination (asterisk) are observed in the lateral membrane domain (region between arrows) of >30% of contacting cells, as opposed to 5% in wild type. Bars: (B and D) 50 nm; (F and G) 400 nm; (A, C, and E) 100 nm.

tal clusters/cell–cell contact occur in wild-type animals as compared with 8.3 (SD 3.2) in *Gli* mutants. The distribution of septa in *Gli* mutants, resembles that reported for stage 14 embryos, suggesting that Gli is necessary for the maturation of pSJs (Tepass and Hartenstein, 1994).

pSJ defects are also observed at tricellular corners (Fig. 4). In wild-type pSJ, septa are typically present at all bicellular contacts of a tricellular junction (Fig. 4 B); however, in *Gli* mutants, pSJ septa are often absent at one or more bicellular contacts, in the region immediately flanking the tricellular channel (Fig. 4 D).

In addition to the pSJ defects observed in *Gli* mutants, gaps between the lateral membranes of adjacent epithelial cells were observed more frequently in wild type (Fig. 4, F and G). 30.4% of cell–cell contacts in *Gli* mutants show large intercellular spaces in the basal portion of the lateral membrane in contrast to (5.1%) in wild type (Fig. 4 G, asterisk). In addition, the gaps are of a smaller size in wild type. These results raise the possibility that Gli may contribute to cell adhesion.

## Transepithelial barriers are compromised in *Gli* mutants

The mislocalization of Dlg, Nrx, and Cora, as well as the abnormal distribution of pSJ septa, in the epidermis of *Gli* mutants, suggests that pSJs are unable to form effective transepithelial barriers in these animals. To test this hypothesis, a dye permeability assay was performed in the salivary glands (Lamb et al., 1998). Gli is localized to the tricellular corners of salivary gland epithelial cells as in the epidermis (Fig. 5, A and B), and overlaps with Cora at pSJs when the gland is viewed in cross section (Fig. 5 C). As in the epidermis, the SJ markers Dlg, Cora, and Nrx are all mislocalized in the salivary glands of *Gli* mutants (unpublished data).

To test the integrity of the pSJ transepithelial barrier in salivary glands, a 10-kD rhodamine–dextran conjugate was injected into the hemocoel of wild-type ($n = 23$) and homozygous $Gli^{\Delta E2\Delta 45}$ mutant ($n = 37$) embryos. In these studies, we were careful to choose stage 17 embryos that are expected to have functional pSJs (Lamb et al., 1998). In all wild-type animals tested, the rhodamine–dextran dye was effectively blocked from passing into the lumen of the salivary gland for up to 40 min after injection (Fig. 5, D–F), after which the animals would hatch and crawl away. In these animals, the dye was able to pass between salivary gland epithelial cells, in a basal to apical direction, up to the pSJ where it stopped without penetrating into the lumen (Fig. 5 E, arrowhead). In contrast, in every *Gli* mutant tested, the tracer dye was found to pass into the salivary gland lumen within 10 min of injection (Fig. 5, G–I). In these animals, the dye was observed to pass between epithelial cells at multiple consecutive cell–cell contacts (Fig. 5, H and I, arrowheads). In a given longitudinal section (2 μm confocal slice) of a salivary gland, tricellular corners are not transected in many consecutive cells due to their small size and position at the corners of these hexagonally shaped cells. Therefore, this result suggests that the dye penetrates pSJ domains, not solely at tricellular corners of epithelial cells in *Gli* mutants, but rather around their circumferences. These findings indicate that

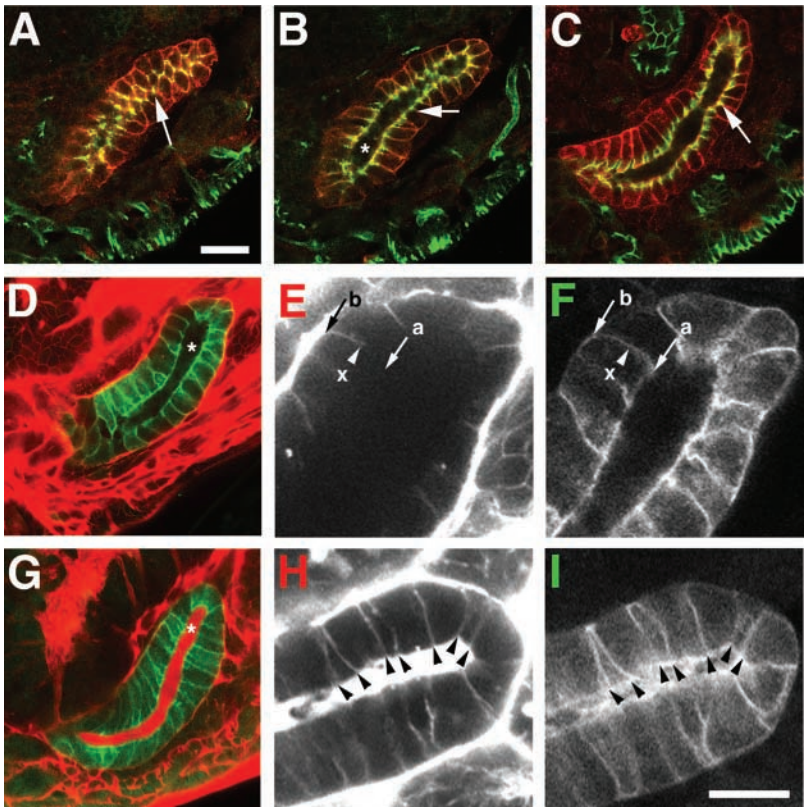


Figure 5. **The integrity of the salivary gland transepithelial barrier is disrupted in *Gli* mutants.** (A–C) Fixed, wild-type, stage 17, *da.G32:UASgapGFP* embryos, stained for gapGFP (red), which marks salivary gland epithelial membranes, and (A and B, green) Gli or (C, green) Cora. Colocalization of gapGFP with Gli or Cora is yellow. (A) Gli is localized to the tricellular corners of salivary gland epithelial cells (en face view) as in the epidermis (arrow). (B) Longitudinal section of the salivary gland shown in A reveals the gland lumen (asterisk) and localization of Gli to the pSJ domain (arrow). (C) Cora labels the apical portion of the lateral membrane similar to Gli (compare arrows in B and C). (D–I) Live, wild-type *da.G32:UASgapGFP* (D–F) and $Gli^{AE2\Delta45}$: *da.G32:UASgapGFP* homozygous mutant (G–I) embryos whose hemocoels have been injected with 10-kD rhodamine–dextran conjugate to evaluate the integrity of the salivary gland transepithelial barrier. Embryos were imaged within 10 min of injection. (D) In wild type, the tracer (red) is excluded from the lumen (asterisk) of the salivary gland, which expresses gapGFP (green). (E) High magnification of the salivary gland (red channel) reveals the tracer, which penetrates between epithelial cells in a basal (b) to apical (a) direction, but only as far as the presumptive pSJ domain (x). Compare position of pSJ domain in C (arrow) with the dye block site (x) in E. (F) Green channel, the dye block site (*x*) is superimposed on the salivary gland epithelial cell profiles. (G) In homozygous *Gli* mutant embryos, the transepithelial barrier function of the salivary gland (green) is impaired and the tracer (red) fills the gland lumen (asterisk). (H and I) In high magnification views of the salivary gland, the tracer (G, red channel) is observed to penetrate between cell–cell contacts of multiple consecutive (arrowheads) epithelial cells. Compare arrowheads in H with those in I (green channel). Bars: (A–D and G) 20 μm; (E, F, H, and I) 10 μm.

the Gli is required for the formation of functional transepithelial barriers.

### Rescue of *Gli* mutants by Gli, but not *Neuroligin* transgenes

To show that pSJ transepithelial barrier defects observed in $Gli^{AE2\Delta45}$ mutants are specifically due to loss of Gli and not due to potential second-site mutations in the genetic background, rescue experiments were performed. We used the GAL4/UAS system (Brand and Perrimon, 1993) to express a wild-type *Gli* transgene (*UAS-*$Gli^{wt}$) in homozygous $Gli^{AE2\Delta45}$ mutant embryos, and then scored for the ability of these rescued embryos to hatch into first instar larvae. A variety of GAL4 drivers were tested. They included, *repoGAL4*, *hsp-G303–7*, and daughterless GAL4 (*da.G32*; Wodarz et al., 1995; Leiserson et al., 2000). Rescue of lethality was obtained with the ubiquitously expressed *da.G32* driver suggesting that there are no second site lethal mutations in the $Gli^{AE2\Delta45}$ mutant strain. In *da.G32:UAS-*$Gli^{wt}$–rescued embryos, Gli localizes correctly to the tricellular corners of epithelial cells in the epidermis (unpublished data). 78% ($n$ = 39) of rescued embryos hatch and survive to adulthood. Rescued adults are fertile and can be maintained as a stable stock, however, 58% ($n$ = 51) have severe leg defects. The metatarsus and tibia are typically bent at 45° toward the midline, and necrotic tissue is often present on the medial aspect of the limbs and limb joints. Similar phenotypes are also seen in adult escapers of a $Gli^{DV5}$ hypomorphic strain (unpublished data), as well as in *Nrx*, and *Cora* hypomorphic mutants (Baumgartner et al., 1996; Lamb et al., 1998). In carrying out the rescue experiments, we were not able to rescue the lethality of homozygous *Gli* mutants with the glial-specific driver *repoGAL4*. This result suggests that the lethality of *Gli* mutants is not solely due to a disrupted glial-based BNB (Auld et al., 1995).

Gli is a member of a large family of cholinesterase-like molecules called the electrotactins, which are structurally very similar to one another (Botti et al., 1998). We wondered if the closest *Drosophila* family member, *Drosophila* neuroligin (Dnl), which has the highest sequence similarity to Gli, of the electrotactins in *Drosophila* (Gilbert et al., 2001), might be functionally similar enough to Gli be interchangeable. Despite that Gli and Dnl share 40% amino acid identity across their extracellular serinesterase-like domains, a Dnl transgene could not rescue *Gli* lethality. These results suggest that Gli and Dnl are not functionally interchangeable electrotactin molecules.

## Discussion

Gli shows a tissue distribution pattern similar to that of the pSJ proteins Cora and Nrx. However, the subcellular distribution of Gli varies from other known pSJ proteins in that Gli is restricted to tricellular junctions. Three lines of evi-

dence suggest that Gli is necessary for pSJ formation. First, the pSJ markers Dlg, Cora, and Nrx are mislocalized in *Gli* mutant epithelial cells. Second, *Gli* mutants do not form effective transepithelial barriers as determined through a salivary gland dye permeability assay. Third, ultrastructural analysis indicates that pSJs are malformed in *Gli* mutants.

The mutant phenotype of *Gli,* in many respects, is similar to that of *Nrx* and *Cora*, however, there are also clear differences between these mutants. In all mutants, SJ markers are mislocalized, but apical–basal polarity appears unaffected. All mutants have dorsal closure defects: whereas in *Nrx* and *Cora* mutants dorsal closure fails, and is accompanied with prominent cuticular defects, in *Gli* mutants, dorsal closure is slightly delayed at a low frequency but eventually completed (Fehon et al., 1994; Baumgartner et al., 1996; Lamb et al., 1998). The most striking difference between *Gli* and *Nrx*/*Cora* mutants is that at the ultrastructural level they have distinct pSJ morphologies. In *Nrx*/*Cora* mutants, septa fail to form (Baumgartner et al., 1996; Lamb et al., 1998), whereas in *Gli* mutants, a normal number of pSJ strands forms, but they are not tightly arrayed (Fig. 4). This suggests that Nrx/Cora are necessary for pSJ strand synthesis, whereas Gli appears to be required for the maturation of the pSJ, which involves the compaction of SJ strands. pSJs in wild-type embryos, at stage 14 of development, have a morphology that resembles those of late stage *Gli* mutants (Tepass and Hartenstein, 1994). Evidently, compaction of pSJ septa is essential to form an effective transepithelial barrier because *Gli* mutants have leaky salivary glands. This result is in agreement with the findings of Swales and Lane (1985), who have shown in locust that tracer dyes are often able to cross individual septa, as well as small groups, but that the wild-type distribution of multiple large groups of septa do form effective permeability barriers. It is also possible that the detachment of lateral membranes observed in *Gli* mutants may contribute to a compromised permeability barrier.

## Gli, SJ development, and the "tricellular plug" (TCP) model

Several ultrastructural studies of various insects, including *Drosophila*, have demonstrated specialized structures at the tricellular corners of epithelial cells that are linked to SJs (Fristrom, 1982; Graf et al., 1982; Lane and Swales, 1982). Graf et al. (1982) performed a detailed freeze-fracture EM analysis of epithelial tissue in crustaceans and cockroaches and identified channels at the tricellular corners of abutting epithelial cells (Fig. 6). These channels span the length of the cells. In the region of the SJ domain, the channels are filled with what appears to be a series of diaphragms that are stacked on top of each other. The diaphragms make contact with the lateral membranes of all three epithelial cells comprising a channel. In the vicinity of the tricellular corners, SJ strands run parallel to the axis of the channel. This organization is different from that of SJ strands elsewhere in the cell. SJ strands typically run parallel to the axis of the apical membrane domain. Graf et al. (1982) suggested that SJ strands anchor on the stacked arrays of diaphragms at tricellular corners. Other researchers referred to these structures as TCPs, and suggested that they serve as occlusive devices during transepithelial barrier formation in

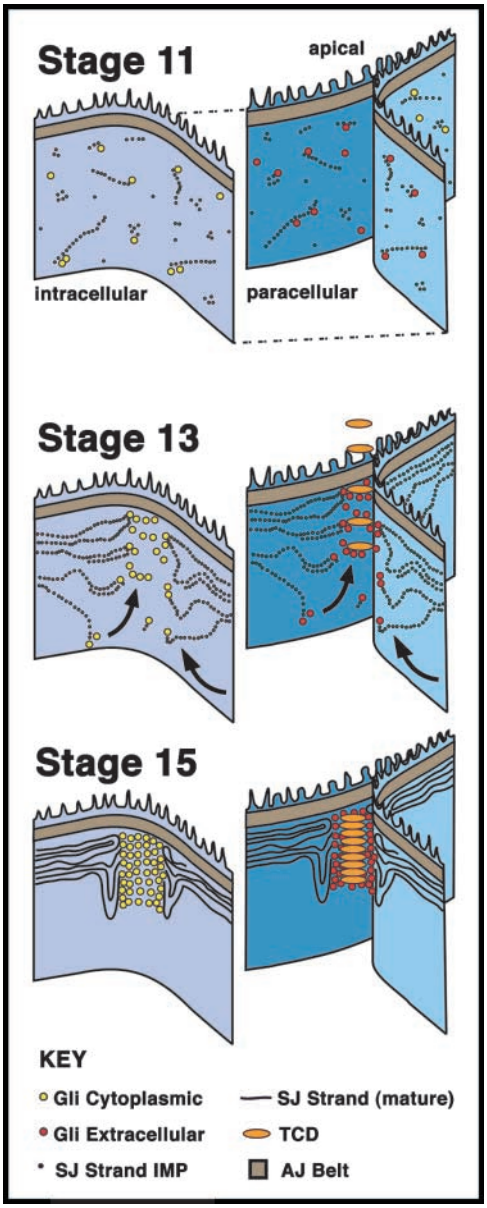


Figure 6. **Model of Gli's role in SJ maturation in the epidermis.** pSJ junction development is depicted at three stages of embryogenesis (stages 11, 13, and 15). For each stage, a tricellular corner is shown with one cell shifted off to the left (dotted lines at stage 11) in order to reveal the paracellular space. The apical membrane domain of the epithelium is denoted with its characteristic projections of microvilli. (Stage 11) Early in pSJ development, pSJ strand IMPs are randomly distributed in the lateral membrane and begin to polymerize into short pSJ strands. IMPs may represent protein complexes containing the transmembrane protein Nrx and various cytosolic proteins (Cora, Dlg, and Scrib). Gli has affinity for IMP components and associates with nascent pSJ strands. (Stage 13) Gli's ligand appears at the tricellular corners of epithelial cells and this draws Gli and associated pSJ strands apically (curved arrows). The ligand may be a secreted protein that diffuses down the tricellular channels (arrow) and/or a component of TCDs. (Stage 15) pSJ strands are compacted apically, and anchored to a stacked array of TCDs through Gli. Together, TCDs, Gli, and pSJ strands form an effective transepithelial barrier.

addition to acting as anchors for SJ strands (Fristrom, 1982; Lane and Swales, 1982).

The development of pSJs occurs in a step wise process (Lane and Swales, 1982). Early in pSJ development, intermembrane particles (IMPs), the building blocks of SJ strands, are homogeneously distributed throughout the lateral membrane. They polymerize at random sites in the lateral membrane (in small depressions) to form short pSJ strands. These, in turn, lengthen and "stack" to form pSJ placodes, which eventually anchor on TCP diaphragms. TCPs are not observed early in pSJ development and, thus, they are believed to be mature features of pSJs. Our observations that Gli is localized to the tricellular corners of epithelial cells, and that it is necessary for pSJ maturation is consistent with this TCP model. The EM images of Graf et al. (1982), which show that TCP diaphragms are associated with pSJ strands in the apical half of tricellular channels, agree with our observations that Gli is restricted to the apical half of tricellular corners. These data suggest that Gli is an integral component of TCPs, a notion that could be confirmed by future immuno-EM experiments.

Combining the TCP model with the EM observations of Lane et al. (1994), and our analysis of Gli, we propose a model to suggest how Gli is involved in the formation of pSJ (Fig. 6). During SJ development, Gli may serve as a linker between SJ strands and tricellular channel diaphragms (TCDs). Gli has the potential to associate with TCDs, through its extracellular domain and with SJ strands through its intracellular tail. Nrx and Cora (and possibly Dlg and Scrib) could be integral components of pSJ strands and may represent the pSJ IMPs reported by Lane et al. (1994). Nrx and Cora behave like IMPs in that they are homogeneously distributed in the lateral membranes during stage 12 of embryogenesis, and are concentrated in the apical half of the lateral membrane at stage 15 (Fehon et al., 1994; Baumgartner et al., 1996; unpublished data). It is possible that Gli could physically associate with Nrx and, thus, be linked to SJ strands, because Gli-like vertebrate neuroligins have been shown to bind to neurexin-1β via their cholinesterase-like domains (Ichtchenko et al., 1995). However, Nrx is more similar to the α-neurexins than the β-neurexins, and the latter is not known to bind neuroligins (Ichtchenko et al., 1995; Tabuchi and Südhof, 2002). Gli and Nrx also fail to interact in S2 cell aggregation assays (Auld et al., 1995; Baumgartner et al., 1996). Alternatively, Gli may associate through its intracellular domain with SJ strands as it contains a COOH-terminal PDZ recognition sequence, and Dlg and Scrib are PDZ domain proteins. Also in vertebrates, it has been shown that PSD-95 (a Dlg-related protein) binds the intracellular tail of various neuroligins (Irie et al., 1997). Irrespective of the mechanism, our results support the notion that Gli is physically associated with SJ strands, as Dlg, Nrx, and Cora fail to be confined to the pSJ domain within the lateral membrane, and pSJ strands are unorganized in *Gli* mutant epithelial cells.

Many interesting questions remain to be addressed regarding the specific role of Gli in TCP and pSJ development. Is Gli only necessary to anchor pSJ strands to TCP diaphragms, or is it also directly involved in the formation of the TCP diaphragms? The molecular nature of the diaphragms is not known. One possibility is that the diaphragms are composed of secreted molecules that are linked via Gli to the pSJ strands (Fig. 6). This linkage may be critical for the compaction of SJ strands.

### Gli, tricellular channels, tight and paranodal junctions

Tricellular channels are not features unique to the insect epithelium. Walker et al. (1985) performed a freeze-fracture EM analysis of vertebrate epithelial tissue, and found the organization of TJs at tricellular corners to be strikingly similar to that of SJs in insects. It will be interesting to determine if any of the vertebrate neuroligins are localized to the tricellular corners of epithelial cells, and if they have a role in TJ maturation similar to Gli's role in SJ development. Of particular interest are human Neuroligins 3 and 4, and rat neuroligins 2 and 3, which are not nervous system–specific and which have a broader tissue distribution than other vertebrate neuroligins (Philibert et al., 2000; Bolliger et al., 2001; Gilbert et al., 2001). Given the structural and molecular similarities between *Drosophila* SJs and mammalian paranodal junctions (Tepass et al., 2001), it will also be interesting to determine if neuroligins, or tricellular junctions are present at axon–glial contacts. However, at least two neuroligins, 1 and 3, are not found at paranodal junctions in mice or rat, rather neuroligin 3 appears to be associated with nonmyelinating Schwann cells (unpublished data).

## Materials and methods

### Fly strains

The wild-type stock, Oregon R, was used as a control in all experiments, except for the transepithelial barrier assay (see below). $Gli^{AE2\Delta45}$ and $Gli^{AE2\Delta4b}$ are *P* element excision deletion alleles and protein nulls (Auld et al., 1995). $Gli^{DV3}$ and $Gli^{CQ1}$ are ethyl methane sulfonate alleles; both contain stop codons in the extracellular domain of Gli and are null alleles (Venema, 2003). The SJ mutant $Nrx^{46}$ is a strong ethyl methane sulfonate allele and putative protein null (Baumgartner et al., 1996). The *da.G32-GAL4* driver is ubiquitously expressed (Wodarz et al., 1995), *hsp-GAL4 303–7* is also ubiquitously expressed, but nonhomogeneously (Leiserson et al., 2000), and *repo-GAL4* is expressed in all glia with exception of the midline glia (Sepp et al., 2001). The Gli-GAL4 driver *J29GAL4#2* and the $UAS\text{-}Gli^{wt}$ reporter line were generated as outlined below (next section). The *J29GAL4#2* driver is expressed in a Gli-like distribution. *UAS-gapGFP*, (Bloomington Stock Center, Indiana University, Bloomington, IN) was used to label cell membranes. *UAS-Neuroligin* was obtained from G. Boulianne (Hospital for Sick Children, Toronto, Canada). Marked balancer chromosomes used for mutant analysis were *CyO, P(ry+*, enwglacZ) and *CyO, P(w+*, actinGFP), and *TM6B,P(w+*, iab-2 [1.7]lacZ),Tb.

### Generation of transgenic lines

For the *J29GAL4#2* driver, 3.7 kb of *Gli*'s 5′ regulatory sequence (BamH1-Xba1 fragment of J29LamdaG5 genomic clone; Auld et al., 1995) was subcloned upstream of the *GAL4* cDNA in a pCasper2A+ *P* element transformation vector (Brand and Perrimon, 1993). For the $UAS\text{-}Gli^{wt}$ line, the 3.9-kb *Gli* cDNA (AE2 7.41; Auld et al., 1995) was subcloned into the EcoR1 site of the pP(UAST) transformation vector (Brand and Perrimon, 1993). Engineered constructs (200 ng/μl) were injected into $w^{1118}$ embryos together with the pπ25.7wcΔ2–3 (400 ng/μl) using standard techniques (Rubin and Spradling, 1982), and insertion lines were isolated and balanced.

### Immunohistochemistry

Antibody staining of embryos was performed as described by Halter et al. (1995). Homozygous *Gli* and *Nrx* mutants were identified with marked balancers (blue or GFP) by staining for a lack of β-galactosidase (β-Gal) or GFP expression. Embryos were staged according to Hartenstein (1993). Stained embryos were mounted in Vectashield (Vector Laboratories), and imaged with a Radiance Plus confocal microscope (40× oil and 63× oil objective lenses, Bio-Rad Laboratories). Single, 2-μm optical slices were

recorded in all experiments. Confocal files were processed with Image-J 1.24 and Adobe Photoshop 5.5. Primary antibodies and the dilutions used for embryo staining were: guinea pig anti-Dlg at 1/300 (Woods and Bryant, 1991), mouse anti-Gli (1F61D4) at 1:1 (Auld et al., 1995), mouse anti–*Drosophila* α-spectrin (3A9) at 1:5 (Developmental Studies Hybridoma Bank, University of Iowa, Iowa City, IA), mouse anti-arm (N2 7A1) at 1:5 (Developmental Studies Hybridoma Bank), mouse anti–β-Gal at 1:500 (Sigma BioSciences), mouse anti-Cora (9C and C615–16B cocktail) at 1:100 (Fehon et al., 1994), rabbit anti-Nrx at 1:200 (Baumgartner et al., 1996), rabbit anti–β-Gal at 1:400 (Cappel, ICN Pharmaceuticals Inc.), rabbit anti-GFP at 1:200 (Abcam Ltd.), and rat anti–DE-cadherin at 1:50 (Oda et al., 1994). All the following secondary antibodies (Molecular Probes) were used at 1:300 dilution: goat anti–guinea pig A488, goat anti–mouse A488 and A568, goat anti–rabbit A488 and A568, and goat anti–rat A488. All the secondary antibodies were highly cross adsorbed, except for the rat secondary. The 1F61D4 mAb was preadsorbed before use, by adding 100 μl of 4-h-old embryos (fixed and blocked) to 900 μl of 1F61D4 containing 10% normal goat serum (Sigma BioSciences) and incubating at 4°C overnight.

### Transepithelial barrier assay

Dye injections were performed as described by Lamb et al. (1998) with the following changes. The salivary glands of wild-type and *Gli* mutant embryos were labeled with gapGFP to facilitate detection using the GAL4/UAS expression system (Brand and Perrimon, 1993). For wild-type embryos, *da.G32* females were mated to *w;UAS-gapGFP/CyO* males. Labeled *Gli* mutant embryos were obtained by crossing *w; Gli$^{AE2\Delta45}$*,UAS-gapGFP/CyO females to *w;Gli$^{AE2\Delta45}$*/CyOactinGFP;*da.G32/TM6,Tb* males. The *da.G32* GAL4 driver is strongly expressed in salivary gland tissue. Crosses were performed at 21°C, and eggs were collected at 1-h intervals, and aged for 24 h to obtain stage 17 embryos. Embryo staging was confirmed by scoring for mouth hooks and prominent trachea. Embryos were then dechorionated and spread on glass microscope slides for sorting using a GFP dissecting scope. Mutant *Gli* embryos of the genotype *w; Gli$^{AE2\Delta45}$*,UAS-gapGFP/Gli$^{AE2\Delta45}$; *da.G32/+* were identified as having brightly fluorescing salivary glands, but lacking *CyOactinGFP* expression. Rhodamine-labeled dextran (10,000 mol wt; Molecular Probes) was reconstituted in dd$H_2O$ to 3 mM.

### Rescue experiment

GAL4 drivers capable of rescuing *Gli* lethality were identified by crossing *Gli$^{AE2\Delta45}$*,UAS-Gli$^{wt}$/CyOactinGFP females with *Gli$^{AE2\Delta45}$*/CyOactinGFP; GAL4 driver/TM6,Tb males at 23°C. Progeny were screened with a GFP dissecting scope for non-GFP first instar larval escapers. For each rescue experiment ~2,000 (mixed genotype) embryos were screened. To quantify the frequency at which *w; Gli$^{AE2\Delta45}$*,UAS-Gli$^{wt}$/Gli$^{AE2\Delta45}$; *da.G32/+* embryos were able to hatch, all progeny of the parental rescue cross were dechorionated and screened with a GFP scope to identify homozygous *Gli* mutants. Embryos of the correct genotype were arrayed on apple juice plates, overlaid with halocarbon oil, and incubated at 23°C until hatching occurred. Percent survival was quantified as the number of first instar larval escapers/total number mutant eggs arrayed.

### EM

For standard transmission EM (TEM), late stage 17 wild-type and *Gli* mutant embryos were injected with fixative according to the protocol of Prokop et al. (1998). Embryos were embedded in Epon-Araldite. For high-pressure freezing and freeze substitution, stage 17 embryos were placed in brass specimen holders, using hexedecene as a support medium, and frozen with a high pressure freezer (model HPM010; BAL-TEC, Liechtenstein). Frozen embryos were transferred to acetone substitution medium (2% OsO4, 8% dimethoxypropane, 0.1% uranyl acetate, and kept at −80°C for 3 d, −20°C for 24 h, 4°C for 2 h, and RT for 2 h. Embryos were washed twice with fresh acetone, and embedded in Spurrs resin (25% resin for 3 h, 50% resin for overnight, 75% resin for 3 h, and 100% resin for overnight). Ultrathin sections were stained after with uranyl acetate and lead citrate, and imaged with a Hitachi 7100 STEM.

We thank M. Bhat, P. Bryant, V. Budnik, R. Fehon, M. Gorczyca, H. Oda, E. Wieschaus, and D. Woods for providing antibodies; M. Bhat, G. Boulianne, W. Leiserson, and H. Keshishian for fly stocks; B. Argiropoulos for embryo injection training; H. Hong for TEM sectioning; M. Pellikka for statistical analysis; and K. Sepp, K. Norman, and C. Roskelley for many helpful discussions and comments on the manuscript.

This work was supported by grants to V.J. Auld from the Canadian Institute of Health Research (MOP42439), and the Howard Hughes Medical Institute (75197-526603). J. Schulte was supported by a studentship from the Rick Hansen Neurotrauma Initiative.

Submitted: 31 March 2003
Revised: 22 April 2003
Accepted: 23 April 2003

## References

Auld, V.J., R.D. Fetter, K. Broadie, and C.S. Goodman. 1995. Gliotactin, a novel transmembrane protein on peripheral glia, is required to form the blood-nerve barrier in *Drosophila*. *Cell.* 81:757–767.

Baumgartner, S., J.T. Littleton, K. Broadie, M.A. Bhat, R. Harbecke, J.A. Lengyel, R. Chiquet-Ehrismann, A. Prokop, and H.J. Bellen. 1996. A *Drosophila* neurexin is required for septate junction and blood-nerve barrier formation and function. *Cell.* 87:1059–1068.

Bhat, M.A., C.R. Jose, Y. Lu, G.P. Garcia-Fresco, W. Ching, M. St. Martin, J. Li, S. Einheber, M. Chesler, J. Rosenbluth, et al. 2001. Axon-glial interactions and the domain organization of myelinated axons requires neurexin IV/Caspr/Paranodin. *Neuron.* 30:369–383.

Bilder, D., and N. Perrimon. 2000. Localization of apical epithelial determinants by the basolateral PDZ protein Scribble. *Nature.* 403:676–680.

Bilder, D., M. Schober, and N. Perrimon. 2003. Integrated activity of PDZ protein complexes regulates epithelial polarity. *Nat. Cell Biol.* 5:53–58.

Bolliger, M.F., K. Frei, K.H. Winterhalter, and S.M. Gloor. 2001. Identification of a novel neuroligin in humans which binds to PSD-95 and has a widespread expression. *Biochem. J.* 356:581–588.

Botti, S.A., C.E. Felder, J.L. Sussman, and I. Silman. 1998. Electrotactins: a class of adhesion protein with conserved electrostatic and structural motifs. *Protein Eng.* 11:415–420.

Boyle, M.E., E.O. Berglund, K.K. Murai, L. Weber, E. Peles, and B. Ranscht. 2001. Contactin orchestrates assembly of the septate-like junctions at the paranode in myelinated peripheral nerve. *Neuron.* 30:385–397.

Brand, A.H., and N. Perrimon. 1993. Targeted gene expression as a means of altering cell fates and generating dominant phenotypes. *Development.* 118:401–415.

Burns, A.R., R.A. Bowden, S.D. MacDonell, D.C. Walker, T.O. Odebunmi, E.M. Donnachie, S.I. Simon, M.L. Entman, and C.W. Smith. 2000. Analysis of tight junctions during neutrophil transendothelial migration. *J. Cell Sci.* 113:45–57.

Carlson, S.D., J.L. Juang, S.L. Hilgers, and M.B. Garment. 2000. Blood barriers of the insect. *Annu. Rev. Entomol.* 45:151–174.

Claude, P., and D.A. Goodenough. 1973. Fracture faces of zonulae occludentes from "tight" and "leaky" epithelia. *J. Cell Biol.* 58:390–400.

Fehon, R.G., I.A. Dawson, and S. Artavanis-Tsakonas. 1994. A *Drosophila* homologue of membrane-skeleton protein 4.1 is associated with septate junctions and is encoded by the *coracle* gene. *Development.* 120:545–557.

Furuse, M., H. Sasaki, K. Fujimoto, and S. Tsukita. 1998. A single gene product, claudin-1 or -2, reconstitutes tight junction strands and recruits occludin in fibroblasts. *J. Cell Biol.* 143:391–401.

Furuse, M., H. Sasaki, and S. Tsukita. 1999. Manner of interaction of heterogeneous claudin species within and between tight junction strands. *J. Cell Biol.* 147:891–903.

Fristrom, D.K. 1982. Septate junctions in imaginal disks of *Drosophila*: a model for the redistribution of septa during cell rearrangement. *J. Cell Biol.* 94:77–87.

Gilbert, M., J. Smith, A.J. Roskams, and V.J. Auld. 2001. Neuroligin 3 is a vertebrate gliotactin expressed in the olfactory ensheathing glia, a growth-promoting class of macroglia. *Glia.* 34:151–164.

Gow, A., C.M. Southwood, J.S. Li, M. Pariali, G.P. Riordan, S.E. Brodie, J. Danias, J.M. Bronstein, B. Kachar, and R.A. Lazzarini. 1999. CNS myelin and sertoli cell tight junction strands are absent in Osp/claudin-11 null mice. *Cell.* 99:649–659.

Graf, F., C. Noirot-Timothée, and C.H. Noirot. 1982. The specialization of septate junctions in regions of tricellular junctions. I. Smooth septate junctions (=continuous junctions). *J. Ultrastruct. Res.* 78:136–151.

Halter, D.A., J. Urban, C. Rickert, S.S. Ner, K. Ito, A.A. Travers, and G.M. Technau. 1995. The homeobox gene *repo* is required for the differentiation and maintenance of glia function in the embryonic nervous system of *Drosophila melanogaster*. *Development.* 121:317–332.

Hartenstein, V. 1993. Atlas of *Drosophila* development. Cold Spring Harbor Laboratory Press, Cold Spring Harbor, NY. 214 pp.

Ichtchenko, K., Y. Hata, T. Nguyen, B. Ullrich, M. Missler, C. Moomaw, and T. Südhof. 1995. Neuroligin 1: a splice site-specific ligand for β-neurexins. *Cell.* 81:435–443.

Irie, M., Y. Hata, M. Takeuchi, K. Ichtchenko, A. Toyoda, K. Hirao, Y. Takai, T.W. Tosahl, and T.C. Sudhof. 1997. Binding of neuroligins to PSD-95. *Science.* 277:1511–1515.

Lamb, R.S., R.E. Ward, L. Schweizer, and R.G. Fehon. 1998. *Drosophila coracle*, a member of the protein 4.1 superfamily, has essential structural functions in the septate junctions and developmental functions in embryonic and adult epithelial cells. *Mol. Biol. Cell.* 9:3505–3519.

Lane, N.J., and L.S. Swales. 1982. Stages in the assembly of pleated and smooth septate junctions in developing insect embryos. *J. Cell Sci.* 56:245–262.

Lane, N.J., G. Martinucci, R. Dallai, and P. Burighel. 1994. Electron microscopic structure and evolution of epithelial junctions. *In* Molecular Mechanisms of Epithelial Cell Junctions: From Development to Disease. S. Citi, editor. R.G. Landes Company, Austin, TX. 23–43.

Leiserson, W.M., E.W. Harkins, and H. Keshishian. 2000. Fray, a *Drosophila* serine/threonine kinase homologous to mammalian PASK, is required for axonal ensheathment. *Neuron.* 28:793–806.

Menco, B.P. 1988. Tight-junctional strands first appear in regions where three cells meet in differentiating olfactory epithelium: a freeze-fracture study. *J. Cell Sci.* 89:495–505.

Menegoz, M., P. Gaspar, M. Le Bert, T. Galvez, F. Burgaya, C. Palfrey, P. Ezan, F. Arnos, and J.A. Girault. 1997. Paranodin, a glycoprotein of neuronal paranodal membranes. *Neuron.* 19:319–331.

Morita, K., M. Furuse, K. Fujimoto, and S. Tsukita. 1999. Claudin multigene family encoding four-transmembrane domain protein components of tight junction strands. *Proc. Natl. Acad. Sci. USA.* 96:511–516.

Noirot-Timothée, C., F. Graf, and C. Noirot. 1982. The specialization of septate junctions in regions of tricellular junctions. II. Pleated septate junctions. *J. Ultrastruct. Res.* 78:152–165.

Oda, H., T. Uemura, Y. Harada, Y. Iwai, and M. Takeichi. 1994. A *Drosophila* homolog of cadherin associated with armadillo and essential for embryonic cell-cell adhesion. *Dev. Biol.* 165:716–726.

Perrimon, N. 1988. The maternal effect of lethal(1)discs-large-1: a recessive oncogene of *Drosophila melanogaster. Dev. Biol.* 127:392–407.

Philibert, R.A., S.L. Winfield, H.K. Sandhu, B.M. Martin, and E.I. Ginns. 2000. The structure and expression of the human neuroligin-3 gene. *Gene.* 246: 303–310.

Poliak, S., L. Gollan, R. Martinez, A. Custer, S. Einheber, L.S. Salzer, J. Trimmer, P. Shrager, and E. Peles. 1999. Caspr2, a new member of the Neurexin superfamily is localized at the juxtaparanodes of myelinated axons and associates with $K^+$ channels. *Neuron.* 24:1037–1047.

Prokop, A., M.D. Martin-Bermudo, M. Bate, and N.H. Brown. 1998. Absence of PS integrins or laminin A affects extracellular adhesion, but not intracellular assembly, of hemiadherens and neuromuscular junctions in *Drosophila* embryos. *Dev. Biol.* 196:58–76.

Rubin, G.M., and A.C. Spradling. 1982. Genetic transformation of *Drosophila* with transposable element vectors. *Science.* 218:348–353.

Rubin, L.L., and J.M. Staddon. 1999. The cell biology of the blood-brain barrier. *Annu. Rev. Neurosci.* 22:11–28.

Sepp, K.J., J. Schulte, and V.J. Auld. 2001. Peripheral glia direct axon guidance across the CNS/PNS transition zone. *Dev. Biol.* 238:47–63.

Swales, L.S., and N.J. Lane. 1985. Embryonic development of glial cells and their junctions in the locust central nervous system. *J. Neurosci.* 5:117–127.

Tabuchi, K., and T.C. Südhof. 2002. Structure and evolution of Neurexin genes: insight into the mechanism of alternative splicing. *Genomics.* 79:849–859.

Tepass, U., and V. Hartenstein. 1994. The development of cellular junctions in the *Drosophila* embryo. *Dev. Biol.* 161:563–596.

Tepass, U., G. Tanentzapf, R. Ward, and R. Fehon. 2001. Epithelial cell polarity and cell junctions in *Drosophila. Annu. Rev. Genet.* 35:747–784.

Tsukita, S., and M. Furuse. 2000. Pores in the wall: claudins constitute tight junction strands containing aqueous pores. *J. Cell Biol.* 149:13–16.

Tsukita, S., M. Furuse, and M. Itoh. 2001. Multifunctional strands in tight junctions. *Nat. Rev. Mol. Cell Biol.* 2:285–293.

Ushkaryov, Y.A., A.G. Petrenko, M. Geppert, and T.C. Südhof. 1992. Neurexins: synaptic cell surface proteins related to the α-latrotoxin receptor and laminin. *Science.* 257:50–56.

Venema, D.R. 2003. The role of gliotactin in planar cell polarity. Ph.D. thesis. University of British Columbia, Vancouver. 244 pp.

Walker, D.C., A. MacKenzie, W.C. Hulbert, and J.C. Hogg. 1985. A re-assessment of the tricellular region of epithelial cell tight junctions in trachea of guinea pig. *Acta Anat. (Basel).* 122:35–85.

Ward, R.E., IV, R.S. Lamb, and R. Fehon. 1998. A conserved functional domain of *Drosophila coracle* is required for localization at the septate junction and has membrane-organizing activity. *J. Cell Biol.* 140:1463–1473.

Wodarz, A., U. Hinz, M. Engelbert, and E. Knust. 1995. Expression of crumbs confers apical character on plasma membrane domains of ectodermal epithelia of *Drosophila*. *Cell.* 82:67–76.

Woods, D.F., and P.J. Bryant. 1991. The discs-large tumor suppressor gene of *Drosophila* encodes a guanylate kinase homolog localized at septate junctions. *Cell.* 66:451–464.

Woods, D.F., C. Hough, D. Peel, G. Callaini, and P.J. Bryant. 1996. Dlg protein is required for junction structure, cell polarity, and proliferation control in *Drosophila* epithelia. *J. Cell Biol.* 134:1469–1482.